

Twisting Neutral Particles with Electric Fields

Niels Geerits^{1*} and Stephan Sponar¹

¹*Atominstitut, Technische Universität Wien, Stadionallee 2, 1020 Vienna, Austria*

(Dated: March 12, 2024)

We demonstrate that spin-orbit coupled states are generated in neutral magnetic spin 1/2 particles travelling through an electric field. The quantization axis of the orbital angular momentum is parallel to the electric field, hence both longitudinal and transverse orbital angular momentum can be created. Furthermore we show that the total angular momentum of the particle is conserved. Finally we propose a neutron optical experiment to measure the transverse effect.

PACS numbers: 03.65.-w, 03.75.Be, 03.65.Vf

I. INTRODUCTION.

Intrinsic orbital angular momentum (OAM) has been observed in free photons [1–3] and electrons [4–6]. Furthermore extrinsic OAM states have also been observed in neutrons, using spiral phase plates [7] and magnetic gradients [8]. In the latter case spin-orbit coupled states are generated [9]. It has also been demonstrated that magnetic quadrupoles can generate spin-orbit states in neutral spin 1/2 particles [10, 11]. The aforementioned methods require a beam with exceptional collimation (0.01° - 0.1° divergence) if intrinsic OAM is the goal. Furthermore the incident particles must be on the optical axis. These two requirements limit the available flux to an impractical level. For this reason intrinsic OAM has not been observed in neutrons to date [12]. The additional quantum degree of freedom offered by OAM provides utility in the realm of quantum information [13–15]. Additionally in neutrons the additional degree of freedom may help improve existing tests of quantum contextuality [16, 17]. Furthermore neutrons carrying net OAM may reveal additional information on atomic nuclei in scattering experiments [18].

In this paper we propose a method by which intrinsic spin-orbit states can be generated in an arbitrarily collimated beam of neutral spin 1/2 particles. This removes flux limitations and allows for the construction of spin-orbit optical equipment for neutrons. We show that a static homogeneous electric field polarized along the direction of particle propagation induces longitudinal spin-orbit states, while a transversely polarized electric field generates transverse spin-orbit states. The latter type of OAM has not yet been observed in massive free particles. Furthermore we confirm previous results that the total angular momentum of a particle is conserved in static electric fields [19]. As shown by Schwinger [20] in an electric field the particle spin couples to the cross product between the electric field strength and the particle momentum. Phase shifts due to this coupling

have been observed in Schwinger scattering [21–24], the Aharonov Casher effect [25–27] and in measurements of the neutron electric dipole moment [28–31] where it can be a major systematic effect. In dynamical diffraction from non-centrosymmetric crystals spin rotations of up to 90° have been observed [23, 30], due to large interplanar fields. Recently the Schwinger coupling has been used to image electric fields with polarized neutrons [32]. However to date no tests for OAM have been conducted.

II. THEORETICAL FRAMEWORK.

An observer moving through an electric field, E , will experience a magnetic field B' . In the low velocity limit when $v \ll c$ the magnetic field can be written as [33]

$$\vec{B}' = \vec{v} \times \frac{\vec{E}}{c^2} \quad (1)$$

Inversely in the lab frame a moving magnetic moment will appear to have a small electric dipole moment $\vec{d}' = \frac{\vec{v} \times \vec{\mu}}{c^2}$. Hence a spin 1/2 particle with magnetic moment $\vec{\mu}$ experiences a Zeeman shift $\vec{d}' \cdot \vec{E} = \vec{\mu} \cdot \vec{B}'$ when moving through an electric field. Therefore the Schroedinger equation is

$$[-\nabla^2 - \frac{\gamma}{c^2} \vec{\sigma} \cdot (\vec{p} \times \vec{E})]\psi = \epsilon\psi \quad (2)$$

with γ the gyromagnetic ratio and $\vec{\sigma}$ the Pauli matrices. The wavefunction is described by a spinor $\psi = \begin{pmatrix} \psi_+(x, y, z) \\ \psi_-(x, y, z) \end{pmatrix}$, where the index \pm refers to the spin state parallel or anti-parallel to the z-axis respectively.

A. Transmission Geometry - Longitudinal OAM.

First we will consider the longitudinal spin-orbit effect. We will assume that the extent of the electric field is semi-infinite and that it is parallel to the z-axis. Hence the Schroedinger equation can be written as

$$-\nabla^2 \psi_{\pm} + iC \left(\frac{\partial}{\partial y} \pm i \frac{\partial}{\partial x} \right) \psi_{\mp} = \epsilon \psi_{\pm} \quad (3)$$

* niels.geerits@tuwien.ac.at

with $C = \frac{\gamma E_z}{c^2}$. The incident wave will be described by $\psi_{\pm}^I = f(r, \phi)e^{-ik_z z}$. Note that for a non-zero coupling this effect requires the incident wavefunction to have a transverse momentum component. By applying a Fourier transform over the x and y coordinates the PDE (Eq. 3) is simplified to a coupled second order ODE.

$$-\left(\frac{\partial^2}{\partial z^2} - k_r^2 + \epsilon\right)\hat{\psi}_{\pm} \mp iCk_r e^{\mp i\phi}\hat{\psi}_{\mp} = 0 \quad (4)$$

Here we have also transformed the equation to cylindrical coordinates with $k_r^2 = k_x^2 + k_y^2$ and $k_x \pm ik_y = k_r e^{\pm i\phi}$. It is noteworthy that in the spectral domain the potential, $C(k_x \sigma_y + k_y \sigma_x)$, closely resembles that of the magnetic quadrupole in real space. This gives an intuitive reason as to why a static electric field mimics the action of a quadrupole in reciprocal space. Hence an electric field is more effective for large divergences (i.e. large k_r). We diagonalize equation 4, by applying a transformation of the form $\hat{\psi} = T\hat{\psi}'$ and multiplying the Hamiltonian by T^{-1} from the left.

$$[-(\frac{\partial^2}{\partial z^2} - k_r^2 + \epsilon) \mp Ck_r]\hat{\psi}'_{\pm} = 0 \quad (5)$$

For this particular diagonalization T is given by $\begin{pmatrix} ie^{-i\phi} & -ie^{-i\phi} \\ 1 & 1 \end{pmatrix}$. The general solution to Eq. 5 is simply a superposition of a forward and backward propagating plane wave for each spin state

$$\hat{\psi}' = \begin{pmatrix} \hat{t}_1 e^{ik_+ z} + \hat{t}_2 e^{-ik_+ z} \\ \hat{t}_3 e^{ik_- z} + \hat{t}_4 e^{-ik_- z} \end{pmatrix} \quad (6)$$

with $k_{\pm} = \sqrt{\epsilon - k_r^2 \pm Ck_r}$. Amplitudes of the backward propagating solutions, \hat{t}_1 and \hat{t}_3 , are zero. The general solution for $\hat{\psi}$ is simply found by applying the transformation $T\hat{\psi}'$.

$$\hat{\psi} = \begin{pmatrix} ie^{-i\phi}[\hat{t}_2 e^{-ik_+ z} - \hat{t}_4 e^{-ik_- z}] \\ \hat{t}_2 e^{-ik_+ z} + \hat{t}_4 e^{-ik_- z} \end{pmatrix} \quad (7)$$

To determine the values of \hat{t}_2 , \hat{t}_4 and the reflection coefficients \hat{r}_{\pm} we apply the boundary conditions

$$\begin{aligned} \hat{\psi}(k_r, \phi, z=0) &= \hat{f}_{\pm} + \hat{r}_{\pm} \\ \hat{\psi}_z(k_r, \phi, z=0) &= ik_z(\hat{r}_{\pm} - \hat{f}_{\pm}) \end{aligned} \quad (8)$$

Here the subscript z under ψ denotes the partial derivative to the z coordinate. $\hat{f}_{\pm}(k_r, \phi)$ denotes the 2D Fourier transform of the incident wavefunction. This boundary value problem can be formulated as the following matrix vector problem

$$\begin{pmatrix} 1 & -1 & 1 & 0 \\ 1 & 1 & 0 & -1 \\ k_+ & -k_- & -k_z & 0 \\ k_+ & k_- & 0 & k_z \end{pmatrix} \begin{pmatrix} \hat{t}_2 \\ \hat{t}_4 \\ i\hat{r}_+ e^{i\phi} \\ \hat{r}_- \end{pmatrix} = \begin{pmatrix} -i\hat{f}_+ e^{i\phi} \\ \hat{f}_- \\ -ik_z \hat{f}_+ e^{i\phi} \\ k_z \hat{f}_- \end{pmatrix} \quad (9)$$

By inverting the above 4x4 matrix we find the transmission and reflection coefficients

$$\begin{aligned} \hat{t}_{(4)}^{(2)} &= \frac{\mp ik_z \hat{f}_+ e^{i\phi} + k_z \hat{f}_-}{(k_z + k_{\pm})} \\ \hat{r}_{\pm} &= \pm \frac{(k_z^2 - k_+ k_-) \hat{f}_{\pm} \mp ik_z (k_+ - k_-) e^{\mp i\phi} \hat{f}_{\mp}}{(k_+ + k_z)(k_- + k_z)} \end{aligned} \quad (10)$$

which leads us to the solution for the transmitted waves

$$\hat{\psi}_{\pm} = \frac{k_z \hat{f}_{\pm} \pm ik_z \hat{f}_{\mp} e^{\mp i\phi}}{(k_z + k_+)} e^{-ik_+ z} + \frac{k_z \hat{f}_{\pm} \mp ik_z \hat{f}_{\mp} e^{\mp i\phi}}{(k_z + k_-)} e^{-ik_- z} \quad (11)$$

Looking at this expression we can see that the total angular momentum $J = S + L$ of the wave is conserved in a static electric field, since a spin flip is compensated by a change in OAM.

$\hat{f}_{\pm}(k_r, \phi)$ can be expanded such that $\hat{f}_{\pm}(k_r, \phi) = \sum_{\ell} \hat{f}_{\pm}^{\ell}(k_r) e^{i\ell\phi}$, where $\hat{f}_{\pm}^{\ell}(k_r)$ is given by the azimuthal Fourier Transform

$$\hat{f}_{\pm}^{\ell} = \int_0^{2\pi} \hat{f}_{\pm}(k_r, \phi) e^{-i\ell\phi} d\phi \quad (12)$$

The solution in real space can be obtained by applying the Bessel/Hankel transform to Eq. 11.

$$\begin{aligned} \psi_{\pm} &= \sum_{\ell} i^{-\ell} k_z e^{i\ell\theta} \\ &\int_0^{\infty} \frac{\hat{f}_{\pm}^{\ell} \pm i\hat{f}_{\mp}^{\ell\pm 1}}{(k_z + k_+)} e^{-ik_+ z} + \frac{\hat{f}_{\pm}^{\ell} \mp i\hat{f}_{\mp}^{\ell\pm 1}}{(k_z + k_-)} e^{-ik_- z} J_{\ell}(k_r r) k_r dk_r \end{aligned} \quad (13)$$

It is instructive to look at the solution of Eq. 13 for an incident wavefield, ψ_{\pm}^I , described by a Bessel beam carrying no OAM, $\psi_{\pm}^I = b_{\pm} J(k_{\rho} r) e^{-ik_z z}$, with b_{\pm} the amplitude of the up and down spin state respectively and k_{ρ} the transverse momentum component of the incident wave. Hence $\hat{f}_{\pm}^{\ell \neq 0} = 0$ and $\hat{f}_{\pm}^0(k_r) = b_{\pm} \frac{\delta(k_r - k_{\rho})}{k_r}$ with $\epsilon = k_z^2 + k_{\rho}^2$. In this case the solution is trivial

$$\begin{aligned} \psi_{\pm}^0 &= k_z b_{\pm} J_0(k_{\rho} r) \left(\frac{e^{-i\sqrt{k_z^2 + Ck_{\rho}} z}}{(k_z + \sqrt{k_z^2 + Ck_{\rho}})} + \frac{e^{-i\sqrt{k_z^2 - Ck_{\rho}} z}}{(k_z + \sqrt{k_z^2 - Ck_{\rho}})} \right) \\ \psi_{\pm}^1 &= \pm k_z b_{\mp} J_1(k_{\rho} r) \left(\frac{e^{-i\sqrt{k_z^2 + Ck_{\rho}} z}}{(k_z + \sqrt{k_z^2 + Ck_{\rho}})} - \frac{e^{-i\sqrt{k_z^2 - Ck_{\rho}} z}}{(k_z + \sqrt{k_z^2 - Ck_{\rho}})} \right) \end{aligned} \quad (14)$$

where ψ_{\pm}^0 and ψ_{\pm}^1 are the components with and without OAM respectively, such that $\psi_{\pm} = \psi_{\pm}^0 + e^{\mp i\theta} \psi_{\pm}^1$. For a collimated beam geometry we may use $k_{\rho} = k_z \tan(\alpha) \approx k_z \alpha$, where α is the beam divergence. Furthermore if Ck_{ρ} is sufficiently small we may linearize the square root terms in equation 14 and obtain a much simpler expression for the wavefunction.

$$\begin{aligned} \psi_{\pm} &= [b_{\pm} \cos(\frac{\gamma E_z \alpha}{2c^2} z) J_0(k_{\rho} r) \\ &\pm b_{\mp} \sin(\frac{\gamma E_z \alpha}{2c^2} z) e^{\mp i\theta} J_1(k_{\rho} r)] e^{-ik_z z} \end{aligned} \quad (15)$$

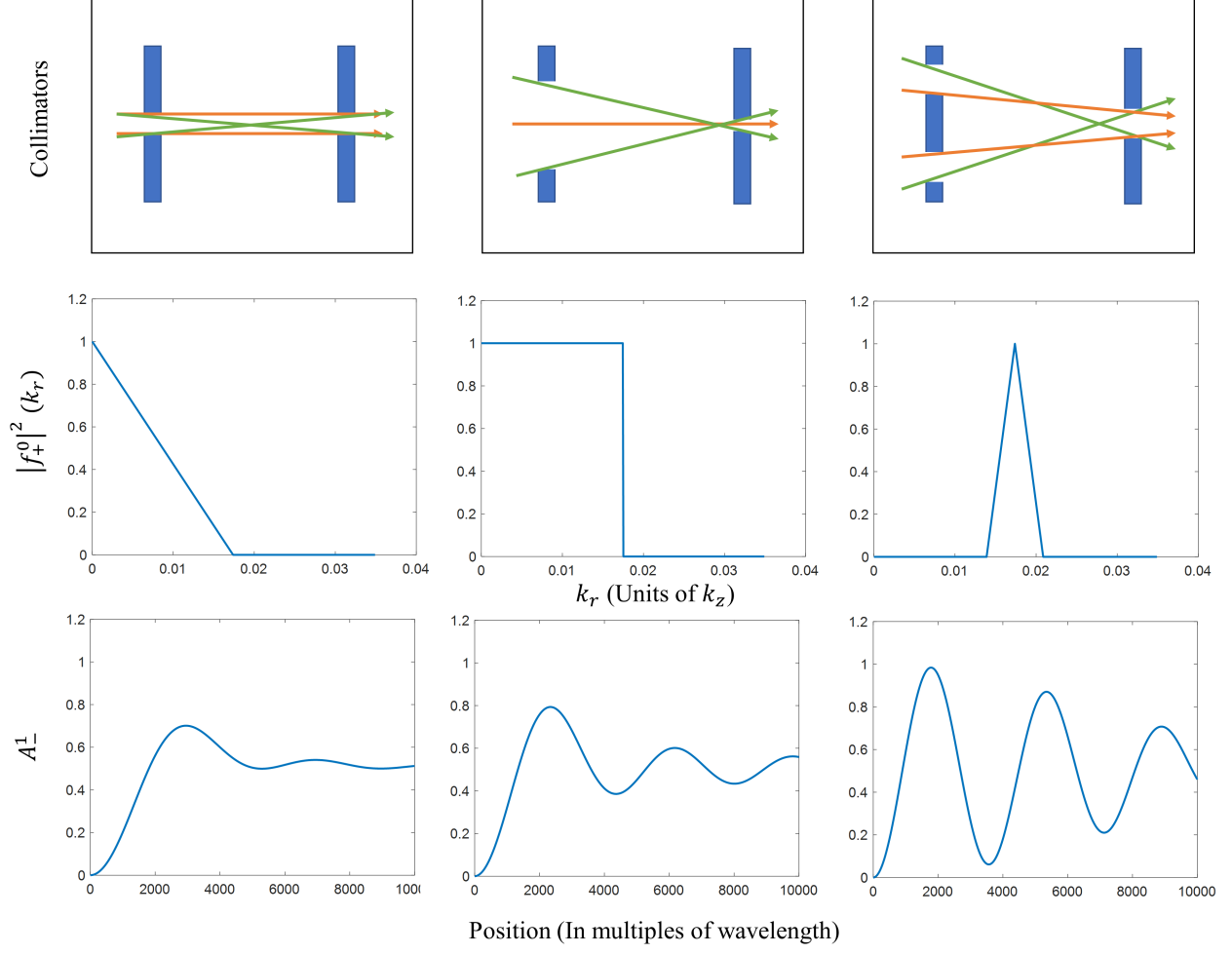


FIG. 1. For various common collimator types such as two identical pinholes (left), a large exit and a comparatively small pinhole (middle) and an annulus with pinhole (right), we show the possible beam paths through a hypothetical instrument (top) and the respective divergence profiles (middle). The paths with the lowest divergence are drawn in orange, while the maximum divergence paths are shown in green. The divergence profiles are used as $|f_+|^2(k_r)$ in equation 17 to determine the probability of finding the particle in the $l = 1$ OAM state as a function of the z position in an electric field (bottom). The parameters are chosen such that $k_z = 1$, $\epsilon \approx k_z^2$ and $C = 0.1$. We note that that in a real instrument these divergence profiles might represent the incoherent average of all possible incident wavefields and not the actual transverse incident wavefield of a single neutron.

A longitudinal beam twister device may be constructed using a parallel plate capacitor, with the surfaces of the plates normal to the beam. The voltage required to fully twist the beam from the $\ell = 0$ state into the $\ell = \pm 1$ state is given by

$$V = \frac{\pi c^2}{\gamma \alpha} \quad (16)$$

These equations are valid for single Bessel beams. However Bessel functions are not normalizable [34] and therefore have infinite coherence, making them unphysical. In a realistic setup we always have a normalizable superposition of Bessel beams, which have finite coherence. This superposition interferes and results in damping of spin

orbit production, due to dephasing. This interference can be described by solving Eq. 13 for an arbitrary divergence profile. Though we can also determine the probability of the particle being in the m th OAM state as a function of z without the inverse transform, Eq. 13, by simply calculating the projection of Eq. 11 on $e^{im\phi}$ and integrating the absolute value squared of this expression over k_r :

$$A_{\pm}^m = \int |\hat{\psi}_{\pm}^m|^2 k_r dk_r = \int |\psi_{\pm}^m|^2 r dr \quad (17)$$

with $\hat{\psi}^m = \langle e^{im\phi} | \hat{\psi} \rangle$, the azimuthal Fourier transform (eq. 12) of $\hat{\psi}$. Here we have also used Parseval's theorem to demonstrate that the value of A^m is the same in real

and reciprocal space. Solutions of equation 17 for the most common divergence profiles, $|f|^2(k_r, \phi)$ are shown in figure 1. Here we see dephasing effects which causes the contrast of A_-^1 to wash out as the wave penetrates deeper into the electric field. As the transverse wavelength spread is decreased the dephasing effects are also reduced. This is analogous to dephasing seen in magnetic spin echo instruments, due to the longitudinal wavelength spread [35].

Equation 16 demonstrates that for particles with a divergence of 1° propagating through a capacitor we require a voltage drop of $88.4GV$ to put a neutron into an OAM state with $\ell = \pm 1$. Obviously this is not feasible. For colder particles it is possible to use zone plates which consist of concentric rings of periodically spaced absorber material to increase the transverse momentum, k_r , thereby decreasing the required voltage drop. Such Fresnel lenses have been produced for the purpose of imaging with very cold neutrons [36].

B. Reflection Geometry - Quasi Transverse OAM.

Next we consider waves interacting with an electric field interface at grazing incidence angles. This results in a more pronounced coupling, due to a larger k_r and a smaller value for k_z . The OAM carried by the transmitted and reflected waves in this case is quasi-transverse to the wavevector \vec{k} . Since the quantization axis of the OAM is normal to interface, the incident wave must be described by an infinite superposition of OAM modes. Nonetheless the mean OAM of the transmitted and reflected waves can be raised or lowered by one unit of \hbar with respect to the incident OAM. The reflection probability $|r_\pm|^2$ as a function of incident angle is shown in Fig. 2, for an electric field of $10^{10}V/m$ (found in electric double layers [37, 38]), a neutron wavelength of 2 \AA and an initial spin aligned along the $-z$ direction. We can deduce that the optimal angle of reflection is around 0.001° . Hence this method of OAM generation is likely not feasible due to flux limitations.

C. Transmission Geometry - Transverse OAM

The flux limitations can be overcome by considering transmission through a transversely polarized electric field which leads to the generation of transverse spin-orbit states. To demonstrate this we consider the time dependent Schrodinger equation for a neutral spin $1/2$ particle in an electric field

$$[-\nabla^2 - \frac{\gamma}{c^2} \vec{\sigma} \cdot (\vec{p} \times \vec{E})]\psi = -i\frac{\partial}{\partial t}\psi \quad (18)$$

Again we will assume that the electric field is polarized along the z-direction. However this time we will consider a field which extends infinitely in space. To reduce the problem to an ordinary differential equation we apply an

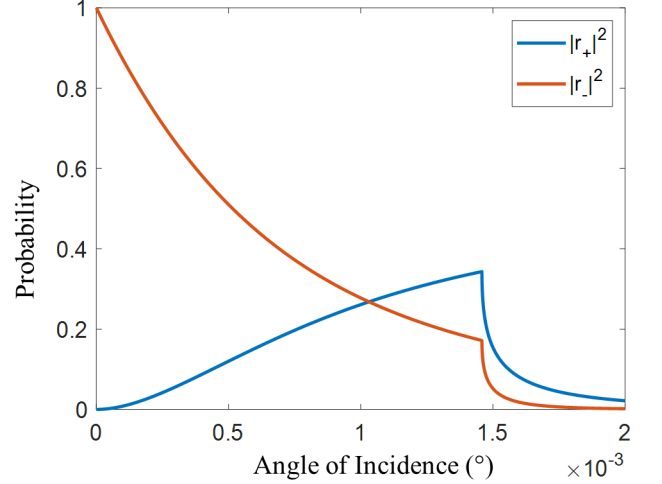


FIG. 2. Reflection probability according to equation 10, $\hat{f}_+ = 0$ and $\hat{f}_- = 1$. A wavelength of 2 \AA and an electric field of $10^{10}V/m$ are assumed. The blue curve corresponds to a spin flip reflection which generates OAM, while the red curve shows the non spin flip reflection probability.

unbounded Fourier transform to the spatial coordinates. In cylindrical coordinates this leads to

$$\epsilon \hat{\psi}_\pm \mp i C k_r e^{\mp i \phi} \hat{\psi}_\mp = -i \frac{\partial}{\partial t} \hat{\psi}_\pm \quad (19)$$

ϵ now denotes the kinetic energy parameter $k_r^2 + k_z^2$. Once again we diagonalize this set of equations using the transform $\hat{\psi} = T \psi'$

$$[\epsilon \mp C k_r] \hat{\psi}'_\pm = -i \frac{\partial}{\partial t} \hat{\psi}'_\pm \quad (20)$$

Applying the initial conditions $\hat{\psi}_\pm(t=0) = \hat{a}_\pm(k_r, \phi, k_z)$ we can determine the homogeneous solution of equation 19.

$$\hat{\psi}_\pm = e^{i \epsilon t} [a_\pm \cos(C k_r t) \pm a_\mp \sin(C k_r t) e^{\mp i \phi}] \quad (21)$$

which appears almost equivalent to equation 15. If the wave propagates along the y-direction the value of k_r , which may be approximated by k_y is a factor $10^2 - 10^3$ larger than in the longitudinal case (equation 15). Hence the required electric field integral to raise or lower the mean OAM is reduced to a more practical level. The incident wave in this case must be described by an infinite superposition of transverse OAM modes. Upon being transmitted through an ideal beam twister device the mean ℓ value of this superposition will be raised or lowered by one. In this paper we assume that \hat{a}_\pm can be approximated by a Gaussian model. The standard deviation in k_x direction can be expressed in terms of a symmetry factor R and the standard deviation in k_y direction σ_y : $\sigma_x = R \sigma_y$. Such that $\hat{a}_\pm = e^{-\frac{(k_y - k'_y)^2}{\sigma_y^2}} e^{-\frac{k_x^2}{R^2 \sigma_y^2}}$, with k'_y , the mean momentum

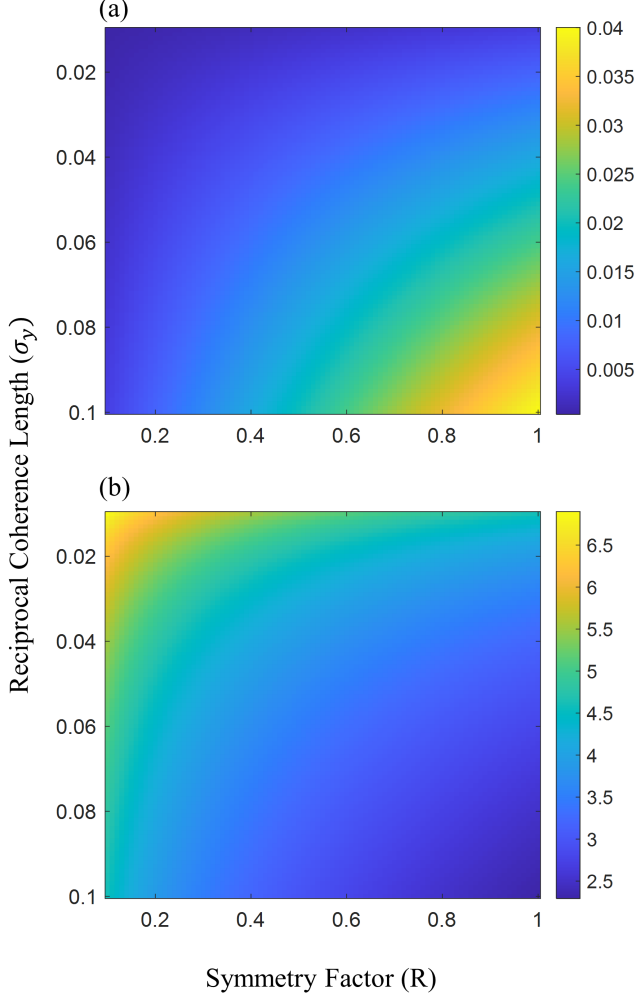


FIG. 3. (a) The amplitude of the first OAM mode A^1 and (b) the logarithm of the OAM bandwidth σ_ℓ of a twisted Gaussian wavepacket plotted as a function of the reciprocal coherence length, σ_y and the symmetry factor R , assuming $k'_y = 1$.

in the y-direction. This Gaussian can be expanded in its various OAM components by means of the azimuthal Fourier transform. Upon passing through an appropriate electric field the index ℓ is raised or lowered by 1. Using this and equation 17 the amplitude of the $\ell = 1$ OAM mode, A^1 , can be calculated. We may also define an OAM bandwidth in terms of the standard deviation

$$\sigma_\ell = \sqrt{\langle L_z^2 \rangle - \langle L_z \rangle^2} \quad (22)$$

with $\langle L_z \rangle = \sum_\ell \ell A^\ell$ and $\langle L_z^2 \rangle = \sum_\ell \ell^2 A^\ell$. Both the OAM amplitude A^1 and the OAM bandwidth, σ_ℓ , are shown as a function of the reciprocal longitudinal coherence length σ_y and the symmetry factor R in Fig. 3. One can see that a small coherence length (large σ_y) leads to a larger amplitude, A^1 and a tighter bandwidth, σ_ℓ . Analogously a large symmetry factor R corresponds (i.e. a large beam divergence) to a larger amplitude, A^1 and a small bandwidth, σ_ℓ .

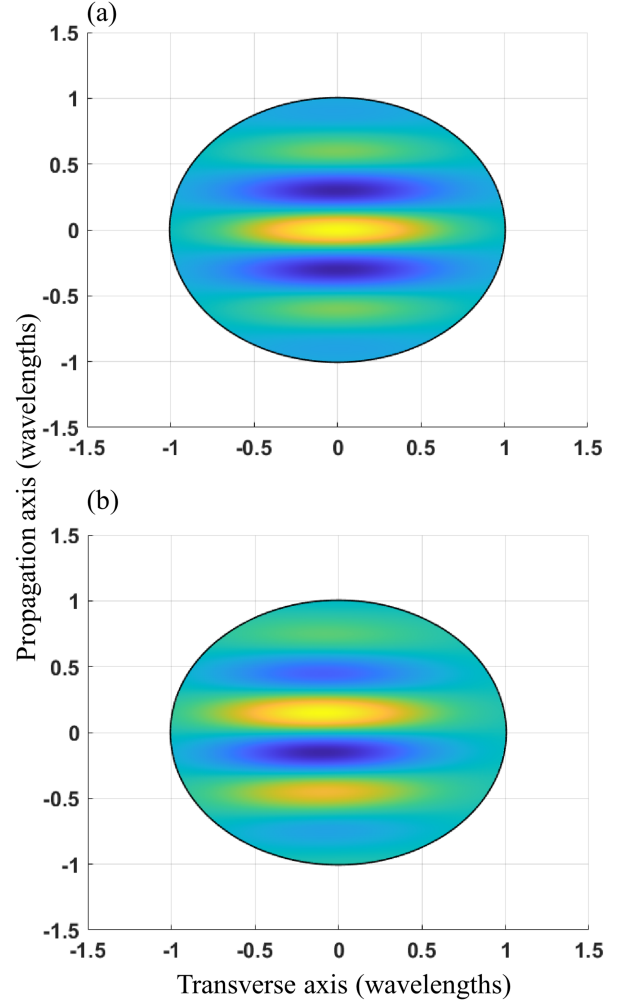


FIG. 4. Surface plots of the real parts of Gaussian wavepackets in real space, with $k'_y = 1$, $\sigma_y^2 = 0.1$ and $R = 1$ carrying (a) no orbital angular momentum and (b) one unit of transverse orbital angular momentum.

In Fig. 4 we show one such Gaussian wavepacket carrying transverse OAM in real space. The wavepacket with OAM appears to be displaced along the transverse axis, while along the longitudinal axis the wavepacket is shifted by $\pi/2$.

III. PROPOSED METHODOLOGY.

Based on the previous theoretical analysis we propose a proof of concept experiment with neutrons to demonstrate that magnetic neutral spin 1/2 particles can obtain quanta of transverse OAM when traversing an electric field polarized perpendicular to the flight direction. The beam twister device will consist of a one meter long evacuated flight tube loaded with two electrodes 1 mm apart. A voltage is applied across the electrodes to generate the experimentally highest possible field in a

- New J. Phys* 20, 103012 (2018).
- [10] E.A. Hinds and C.Eberlein, Quantum propagation of neutral atoms in a magnetic quadrupole guide, *Phys. Rev. A* 61, 033614 (2000).
 - [11] J. Nsofini, D. Sarenac, C.J. Wood, D.G. Cory, M. Arif, C.W. Clark, M.G. Huber, and D.A. Pushin, Spin-orbit states of neutron wave packets, *Phys. Rev. A* 94, 013605 (2016).
 - [12] R. Cappelletti, T. Jach, and J. Vinson, Intrinsic orbital angular momentum states of neutrons, *Phys. Rev. Lett.* 120, 090402 (2018).
 - [13] G. Vallone, V. D'Ambrosio, A. Sponselli, S. Slussarenko, L. Marrucci, F. Sciarrino, and P. Villoresi, Free-space quantum key distribution by rotation-invariant twisted photons, *Phys. Rev. Lett.* 113, 060503 (2014).
 - [14] R. Fickler, R. Lapkiewicz, M. Huber, M.P.J. Lavery, M.J. Padgett, and A. Zeilinger, Interface between path and orbital angular momentum entanglement for high-dimensional photonic quantum information, *Nat. Commun.* 5, 4502 (2014).
 - [15] D. Ding, M. Dong, W. Zhang, Y. Yu, S. Shi, Y. Ye, G. Guo, and B. Shi, Broad spiral bandwidth of orbital angular momentum interface between photon and memory, *Nat. Commun. Phys.* 2, 100 (2019).
 - [16] Y. Hasegawa, R. Loidl, G. Badurek, K. Durstberger-Rennhofer, S. Sponar, and H. Rauch, Engineering of triply entangled states in a single-neutron system, *Phys. Rev. A* 81, 032121 (2010).
 - [17] J. Shen, S.J. Kuhn, R.M. Dalgliesh, V.O. de Haan, N. Geerits, A.A.M. Irfan, F. Li, S. Lu, S.R. Parnell, J. Plomp, A.A. van Well, A. Washington, D.V. Baxter, G. Ortiz, W.M. Snow, and R. Pynn, Unveiling contextual realities by microscopically entangling a neutron, *Nat. Commun.* 11, 930 (2020).
 - [18] A.V. Afanasev, D.V. Karlovets, and V.G. Serbo, Schwinger scattering of twisted neutrons by nuclei, *Phys. Rev. C* 100, 051601 (2019).
 - [19] S.A. Bruce and J.F. Diaz-Valdes, Neutron interaction with electromagnetic fields: a didactic approach, *Eur. J. Phys.* 41, 045402 (2020).
 - [20] J. Schwinger, On the polarization of fast neutrons, *Phys. Rev.* 73, 407-409 (1948).
 - [21] C.G. Shull and R.P. Ferriert, Electronic and nuclear polarization in vanadium by slow neutron scattering, *Phys. Rev. Lett.* 10, 295-297 (1963).
 - [22] C.G. Shull, Neutron spin-neutron orbit interaction with slow neutrons, *Phys. Rev. Lett.* 10, 297-298 (1963).
 - [23] V.V. Voronin, E.G. Lapin, S.Yu. Semenikhin, and V.V. Fedorov, Depolarization of a Neutron Beam in Laue Diffraction by a Noncentrosymmetric Crystal, *J. Exp. Theor. Phys.* 72, 308-311 (2000).
 - [24] T.R. Gentile, M.G. Huber, D.D. Koetke, M. Peshkin, M. Arif, T. Dombeck, D.S. Hussey, D.L. Jacobson, P. Nord, D.A. Pushin, and R. Smither, Direct observation of neutron spin rotation in bragg scattering due to the spin-orbit interaction in silicon, *Phys. Rev. C* 100, 034005 (2019).
 - [25] Y. Aharonov and A. Casher, Topological quantum effects for neutral particles, *Phys. Rev. Lett.* 53, 319-321 (1984).
 - [26] A. Cimmino, G.I. Opat, A.G. Klein, H. Kaiser, S.A. Werner, M. Arif, and R. Clothier, Observation of the topological aharonov-casher phase shift by neutron interferometry, *Phys. Rev. Lett.* 63, 380-383 (1989).
 - [27] A. Cimmino, B.E. Allman, A.G. Klein, H. Kaiser, and S.A. Werner, High precision measurement of the topological aharonov-casher effect with neutrons, *Nucl. Instrum. Methods Phys. Res. A* 440, 579-584 (2000).
 - [28] W.B. Dress, P.D. Miller, J.M. Pendlebury, P. Perrin and N.F. Ramsey Search for an electric dipole moment of the neutron, *Phys. Rev. D* 15, 9-21 (1977).
 - [29] P.G. Harris, C.A. Baker, K. Green, P. Iaydjiev, S. Ivanov, D.J.R. May, J.M. Pendlebury, D. Shiers, K.F. Smith, M. van der Grinten and P. Geltenbort New Experimental Limit on the Electric Dipole Moment of the Neutron, *Phys. Rev. Lett* 82, 904-907 (1999).
 - [30] V.V. Fedorov, M. Jentschel, I.A. Kuznetsov, E.G. Lapin, E. Lelièvre-Berna, V. Nesvizhevsky, A. Petoukhov, S.Yu. Semenikhin, T.Soldner, V.V. Voronin and Yu. P. Braginetz Measurement of the neutron electric dipole moment via spin rotation in a non-centrosymmetric crystal *Phys. Lett. B* 694, 22-25 (2010).
 - [31] F.M. Piegsa New concept for a neutron electric dipole moment search using a pulsed beam, *Phys. Rev. C* 88, 045502 (2013).
 - [32] Y.Y. Jau, D.S. Hussey, T.R. Gentile and W. Chen, Electric Field Imaging Using Polarized Neutrons, *Phys. Rev. Lett.* 125, 110801 (2020).
 - [33] A. Zangwill, *Modern Electrodynamics*, Cambridge University Press, New York, USA (2013).
 - [34] K.Y. Bliokh, I.P. Ivanov, G. Guzzinati, L. Clark, R. Van Boxem, A. Béch , R. Juchtmans, M.A. Alonso, P. Schattschneider, F. Nori and J. Verbeeck Theory and applications of free-electron vortex states *Phys. Rep.* 690, 1-70 (2017).
 - [35] F. Mezei The principles of neutron spin echo. in *Neutron Spin Echo Lecture Notes in Physics* 128, 1-26 Springer, Berlin, Heidelberg (1980)
 - [36] P.D. Kearney, A.G. Klein, G.I. Opat and R. Gaehler Imaging and focusing of neutrons by a zone plate *Nature* 287, 313-314 (1980).
 - [37] M.F. Toney, J.N. Howard, J. Richer, G.L. Borges, J.G. Gordon, O.R. Melroy, D.G. Wiesler, D. Yee, and L.B. Sorensen, Distribution of water molecules at ag(1 1 1)/electrolyte interface as studied with surface x-ray scattering, *Surf. Sci.* 355, 326-332 (1995).
 - [38] I. Danielewicz-Ferchmin and A.R. Ferchmin, A phase transition in h2o due to a high electric field close to an electrode, *Chem. Phys. Lett.* 351, 397-402 (2002).
 - [39] J. Leach, M.J. Padgett, S.M. Barnett, S. Franke-Arnold, and J. Courtial, Measuring the orbital angular momentum of a single photon, *Phys. Rev. Lett.* 88, 257901 (2002).